Cell. Mol. Life Sci. (2012) 69:1193–1210
DOI 10.1007/s00018-011-0873-5

Cellular and Molecular Life Sciences

RESEARCH ARTICLE

# Differential pathotropism of non-immortalized and immortalized human neural stem cell lines in a focal demyelination model

**Daniela Ferrari · Cristina Zalfa · Laura Rota Nodari · Maurizio Gelati · Luigi Carlessi · Domenico Delia · Angelo Luigi Vescovi · Lidia De Filippis**

Received: 23 June 2011 / Revised: 22 September 2011 / Accepted: 18 October 2011 / Published online: 11 November 2011


**Abstract** Cell therapy is reaching the stage of phase I clinical trials for post-traumatic, post-ischemic, or neurodegenerative disorders, and the selection of the appropriate cell source is essential. In order to assess the capacity of different human neural stem cell lines (hNSC) to contribute to neural tissue regeneration and to reduce the local inflammation after an acute injury, we transplanted GMP-grade non-immortalized hNSCs and v-myc (v-IhNSC), c-myc T58A (T-IhNSC) immortalized cells into the corpus callosum of adult rats after 5 days from focal demyelination induced by lysophosphatidylcholine. At 15 days from transplantation, hNSC and T-IhNSC migrated to the lesioned area where they promoted endogenous remyelination and differentiated into mature oligodendrocytes, while the all three cell lines were able to integrate in the SVZ. Moreover, where demyelination was accompanied by an inflammatory reaction, a significant reduction of microglial cells' activation was observed. This effect correlated with a differential migratory pattern of transplanted hNSC and IhNSC, significantly enhanced in the former, thus suggesting a specific NSC-mediated immunomodulatory effect on the local inflammation. We provide evidence that, in the subacute phase of a demyelination injury, different human immortalized and non-immortalized NSC lines, all sharing homing to the stem niche, display a differential pathotropism, both through cell-autonomous and non-cell autonomous effects. Overall, these findings promote IhNSC as an inexhaustible cell source for large-scale

D. Ferrari and C. Zalfa contributed equally to this work.

The present work was developed at the University of Milano-Bicocca, Department of Biotechnologies and Biosciences, Milan, Italy.

**Electronic supplementary material** The online version of this article (doi:10.1007/s00018-011-0873-5) contains supplementary material, which is available to authorized users.

D. Ferrari (✉) · C. Zalfa · L. Rota Nodari · A. L. Vescovi · L. De Filippis (✉)
Department of Biotechnology and Biosciences, Università Milano Bicocca, Piazza della Scienza 2, 20126 Milan, Italy
e-mail: daniela.ferrari@unimib.it

L. De Filippis
e-mail: lidia.defilippis@unimib.it

C. Zalfa
e-mail: cristinazalfa@yahoo.it

L. Rota Nodari
e-mail: laura.rotanodari@unimib.it

A. L. Vescovi
e-mail: angelo.vescovi@unimib.it

M. Gelati · A. L. Vescovi
Casa Sollievo Della Sofferenza, S. Giovanni Rotondo (FG), Italy

M. Gelati
e-mail: maurizio.gelati@unimib.it

M. Gelati · A. L. Vescovi
Laboratorio Cellule Staminali, Cell Factory e Biobanca, Azienda ospedaliera "Santa Maria", Terni, Italy

L. Carlessi · D. Delia
Department of Experimental Oncology, Fondazione IRCCS Istituto Nazionale Tumori, Milan, Italy
e-mail: luigi.carlessi@istitutotumori.mi.it

D. Delia
e-mail: domenico.delia@istitutotumori.mi.it

preclinical studies and non-immortalized GMP grade hNSC lines as an efficacious, safe, and reliable therapeutic tool for future clinical applications.

**Keywords** Fetal Human Neural Stem Cells · Re-myelination · Transplantation · Lysophosphatidylcoline · Immunomodulation

## Introduction

The identification of cells with stem-like properties in the mammalian central nervous system (CNS), including that of humans, throughout development and adulthood [1–3] elucidated the key role played by neural stem cells (NSC) in adult neurogenesis and CNS homeostasis. However, the ability of endogenous stem cells to spontaneously repair the nervous tissue after brain injuries results often insufficient [4, 5] and current studies are addressed to achieve the integration of functional new neuronal and non-neuronal cells by the mobilization of endogenous cells [6, 7] or by transplantation of exogenous cells from different sources. Given their ability to respond to host environmental cues directing their migration and differentiation along multiple phenotypic pathways [8], NSCs represent optimal candidates for cell therapy of neurodegenerative diseases in humans and this challenge is progressively fostering the establishment of human NSC (hNSC) lines to the clinical stage.

We generated hNSC lines from the telencephalic–diencephalic region of human fetal brain [9–13] under the very same process used for GMP-grade culture conditions. In contrast to their rodent counterpart, hNSCs are resilient to expansion ex vivo, thus strongly limiting their availability for extensive experimental studies. In order to circumvent this issue, we obtained two immortalized hNSC lines, respectively, transduced with v-myc (v-IhNSC) [14, 15] and c-myc T-58A (T-IhNSC) [16]. In vitro, the immortalized cells display a higher self-renewal potential compared to the non-immortalized hNSCs, although retaining a stem-like functional stability and multipotency [14, 16]. In particular, we showed that upon the removal of mitogens hNSC, v-IhNSC and T-IhNSC can generate significant percentages of oligodendrocytes in vitro, with T-IhNSC remarkably prone to early differentiation. These findings supported hNSC and IhNSC as an appealing source of oligodendroglial progenitors for transplantation in animal models of demyelinating disorders. However, most studies have provided compelling evidence that the therapeutic efficacy of hNSC mainly relies on their ability to efficiently engraft into the host tissue, to migrate to the lesion, and to exert a plethora of "healing" actions, such as blunting of toxic molecules, neurotrophic support, and immunomodulation of the local inflammatory environment [17–20], with replacement of damaged cells having a minor effect [21]. Actually, NSC therapy is determined by the synergy between the spontaneous brain remodeling and the proper targeting of transplanted NSCs [22–25]. hNSCs were previously shown to generate large amounts of oligodendroglial progenitors in vivo after pretreatment in vitro with oligodendrogenic factors [26] and to delay the progression of the pathology in non-human primate animal models of multiple sclerosis (MS) after systemic transplantation [25, 27]. In parallel, we proved that v-IhNSCs are able to engraft into the brain of adult rats lesioned by transient global ischemia more efficiently than into the brain of healthy matching controls. v-IhNSC therapeutic efficacy was assessed by their ability to dampen injury-induced microgliosis and astrogliosis, for long-term survival, and to establish functional synaptic junctions with host neuronal cells even under a transient immunosuppression regimen [28].

In this paper, we document the differential ability of hNSC, v-IhNSC, and T-IhNSC lines to engraft in a focal demyelination animal model [29, 30] and to migrate to the lesioned area. Most importantly, we have shown that they are differentially able to promote endogenous repair, to generate oligodendroglial cells, and to modulate the inflammatory environment generated by the lesion.

Moreover, in the perspective of future clinical applications, given the very recent approval of three clinical trials for the exploitation of fetal neural stem cells (StemCells Inc.) in Batten's disease or neuronal ceroid lipofuscinosis (NCL) [31], of fetal neural stem cells (Neuralstem) in ALS patients [32], and of conditionally immortalized neural stem cells (Reneuron) in stroke affected patients [33], for the first time, we compare a non-immortalized hNSC line with v-IhNSC and T-IhNSC lines (the latter analyzed for the first time in vivo) [14]. We show that they display a common tendency to "home" to the SVZ niche, and a different pattern of migration to the lesion site and differentiation, suggesting a diverse "pathotropism". Therefore, the ability to target hNSC fate choice by modulating their intrinsic properties appears as pivotal to the employment of immortalized IhNSC as a tool for the screening of novel drugs and therapeutic protocols in preclinical studies and of non-immortalized clinical-grade hNSC in the therapy of neurodegenerative diseases.

## Materials and methods

### Focal demyelination model

Animal studies were approved by the Ethics Review Committee for Animal Experimentation of the Italian Ministry of Health according to protocol 37/2007B. Adult

female Sprague–Dawley rats (250–275 g) were anesthetized with an intraperitoneal injection of ketamine (60 mg/kg) and xylazine (10 mg/kg).

Lysolecithin (L-α-Palmitoyl-lysophosphatidylcholine, Sigma) was solubilized in PBS solution (2%), 3µl of this solution were injected unilaterally into the rat cc (antero-posterior: −0.3; lateral: +2; dorsoventral: −2.8). The animals were treated with antibiotics and analgesics with daily subcutaneous injections of enrofloxacin 10–15 mg/kg and carprofen 5 mg/kg for 7 days.

### Cell preparation

In this work, we used immortalized cell lines and cell lines derived from a brain specimen obtained, according to the CEAS authorization 13/12/2004 protocol number 7139/05/L, from aborted fetuses. For transplantation, hNSC-P, T-IhNSC-P and v-IhNSC-P neurospheres were mechanically dissociated and seeded ($1 \times 10^4$ cells/cm$^2$) onto laminin (Roche, Basel, Switzerland, http://www.roche-applied-science.com) coated tissue culture flasks (or glass coverslips for immunostaining assay), in FGF2-containing medium (20 ng/ml) for 3 days. The cells were then harvested using versene (Gibco, Auckland, NZ), counted, and resuspended in HBSS (medical) (density of $1 \times 10^5$ cells/µl) and transplanted.

### Western-blot analysis

Immunoblots were performed as described [34]. Cells were washed, pelleted, and lysed in Laemmli buffer containing inhibitors. Aliquots containing 50 µg of protein were size-fractionated on SDS-PAGE and electroblotted onto PVDF membranes (Millipore, Bedford, mass). After blocking with 4% non-fat dried milk, membranes were incubated with monoclonal antibodies for CXCR7, Sox2 (R & D systems), phospho-Tyr1173-EGFR (NanoTools, Germany), vinculin (Sigma, Italy) and with polyclonal antibodies for notch1 (Rockland, PA, USA), PDGFαR (Santa Cruz Biotechnology, Santa Cruz, CA, USA), PDGFβR (upstate) and EGFR (Cell Signaling Technology, Beverly, MA, USA). PVDF membranes were incubated with antibodies in sealed bags using the XBLOT P100 hybridization instrument (Isenet, Milan, Italy). Antibody binding was detected with ECL SuperSignal (Pierce, Rockford, IL), and bands quantitated with ImageQuant.

### Cell transplantation

At 5 days post-injury, rats were anesthetized and stereotactically (David Kopf Instruments, Tujunga, CA) injected with 2.5 µl of each cell suspension (250,000 cells/rat) or HBSS (control rats) into the SVZ close to the lesioned cc (anteroposterior: −0.3; lateral: +1.8; dorsoventral: −2.8). All animals were daily immunosuppressed by subcutaneous injection of cyclosporine A (15 mg/kg; Sandimmun, Novartis).

### Immunohistochemistry and immunocytochemistry

Rats were euthanized with Avertin (300 mg/kg) and transcardially perfused-fixed with 4% paraformaldehyde. Brains were post-fixed overnight, cryoprotected, frozen, and coronally sectioned (18 µm thick) by cryostat. Sections were blocked with 10% normal goat serum (NGS) and 0.3% Triton X-100 for 90 min. Primary antibodies used: human specific nuclei (huN), glial fibrillary acidic protein (GFAP), nestin (nestin), oligodendrocyte marker O4 (O4), Ng2 chondroitin sulfate proteoglycan (Ng2), polysialic acid-neural cell adhesion molecule (PSA-NCAM): Chemicon; huSOX-2, human nestin (huNestin): R&D Systems, Minneapolis, MN; huNotch-1, EGF, CXCL12, CXCR7, CXCR4, huEGFR, pEGFR, PDGFRalpha (see Western blot analysis); PDGF (Novus Biologicals); Neuronal Class III β-TubulinIII, TUJ1 (β-TubIII), myelin basic protein (MBP): Covance; ionized calcium binding adaptor molecule 1 (Iba1, Wako); CD68 (Serotec); NCL-Ki67p (Ki67, Novocastra). The fluorescent secondary antibodies used were labeled with Cy3, Cy2 (Jackson), Alexa Fluor 549 and 488 (Molecular Probes). DAPI (ROCHE) was used as nuclear marker. Labeled samples were analyzed by fluorescence microscopy (Zeiss Axioplan 2 imaging) and by confocal microscopy (Leica DM IRE2).

### Quantification and statistical analysis

The survival rate of transplanted cells was evaluated by counting huN+ cells in serial brain sections (each 20 µm apart) spanning the graft area. The total number of surviving transplanted cells was calculated for the whole graft using the Abercrombie formula [35]. Data are presented as the average percentage of surviving cells over total transplanted cells (250,000).

The antero-posterior migration was calculated by evaluating the distance between the most proximal and most caudal section containing huN+ cells. The maximal medio-lateral migration was calculated by evaluating the distance between the rostral migratory stream and the huN+ cells in the cc, evaluating the section presenting the most lateral migration of cells.

The evaluation of notch+ cells and neural phenotypes derived from transplanted cells was performed by calculating the percentage of huN+ cells co-expressing, respectively, notch, GFAP, β-tubIII, huNestin, Ki67 and Ng2 over the total huN+ cells in three serial sections of the transplanted animals ($n = 3$).

The MBP-delineated area was measured by using AxioVision Rel 4.8 (Carl Zeiss). Values shown represent the average of measurements from three brains per condition ($n = 3$, two sections per rat).

The quantification of microglia activation was obtained by evaluating the antero-posterior and medio-lateral extension of the lesioned brain region containing Iba1+ cells. Quantification of the percentage of Iba1+ cells over total DAPI was performed in four regions of interest per section (cc: corpus callosum, cc/RMS: cc adjacent to the rostral migratory stream, l-SVZ: lateral sub-ventricular zone, v-SVZ: inferior tip of the sub-ventricular zone), on five representative serial sections per animal (each 200 μm apart) spanning the central region of lesion and graft.

The quantification of activated macrophagic microglia was obtained by evaluating the number of CD68+ cells in the CC (lesioned brain region containing the major concentration of Iba1+ cells). Quantification of the percentage of CD68+ cells over total DAPI was performed on five representative serial sections per animal (each 200 μm apart).

Statistical analysis was performed by one-way ANOVA. Data is reported as means ± SEM. Each value represents the average of $n = 5$ animals unless differently stated in the text. Data is considered not statistically significant unless indicated in the figures (* indicates $p < 0.05$, ** indicates $p < 0.01$, *** indicates $p < 0.001$).

## Results

### Focal demyelination

In order to assess the oligodendrogenic capacity of hNSC, T-IhNSC, and v-IhNSC cells in vivo, we first established a focal demyelination rat model, lesioned by a unilateral LPC injection into the cc. This treatment induces a rapid but brief influx of T cells [36] accompanied by the activation of macrophages/microglia and demyelination [37, 38]. Given the inflammatory nature of this kind of injury, we investigated the progression of the lesion during the subacute phase of the lesion, which is at 5 days from the injection: a marked increase of the cell density (Fig. 1a, a1) and reactivity for the astroglial and microglial markers, respectively GFAP (Fig. 1b, b1) and Iba1 (Fig. 1c, c1), were remarkably evident in the cc. Parallel demyelination was evidenced by the reduced number of MBP+ oligodendroglial cells with respect to healthy animals (Fig. 1d, d1). At 20 days from the lesion (DAL), the inflammatory reaction appeared slightly reduced (Fig. 1a2, b2, c2) and the recovery of myelin in progress (Fig. 1d2), while a significant decrease of $\beta$-tubIII+ fibers (12.36 ± 0.48 vs. 18.0 ± 1.73% in sham controls at 20 DAL or vs. 16.91 ± 1.26% in lesioned animals at 5 DAL, $p \leq 0.05$) indicated the concomitant slow and progressive neuronal degeneration (Fig. 1e–e2). We also observed a progressive increase of PSA-NCAM+ and nestin+ cells from 5 to 20 DAL in the SVZ, suggesting an increase of host early neuronal progenitors in the lesioned animals (Fig. 1f–f2) [30].

### hNSC, v-IhNSC, and T-hNSC display a common "homing" to SVZ, but a differential tropism to the lesion in demyelinated rats

Given the hostile inflammatory environment developed soon after injury, we transplanted hNSC-, v-hNSC-, and T-hNSC-derived neural progenitors in the LPC injection site 5 days after lesioning, in order to rapidly contribute to myelin regeneration. At the end of the acute phase of the disease, i.e., 15 days following transplantation, we evaluated the graft efficiency of the different cell lines, which were easily identified by the expression of huN. hNSC were detected in 100% ($n = 8/8$), T-IhNSC in 71.4% ($n = 5/7$), and v-IhNSC in 87.5% ($n = 7/8$) of the animals. In the successfully engrafted transplants, we evaluated the percentage of cell survival. Non-immortalized hNSC displayed an increased survival rate (10.26% ± 1.73, $n = 5$) compared to T-IhNSC (5.398 ± 1.75%, $n = 5$, $p \geq 0.05$) and v-IhNSC (3.31 ± 0.45%, $n = 5$, $p \leq 0.01$) (Fig. 2a). In addition, hNSC also migrated more extensively (graft extension along the antero-posterior axis, 2,840 ± 83.67 μm, $n = 5$) with respect to T-IhNSC (1,160 ±303.32 μm, $n = 5$, $p \leq 0.01$) and v-IhNSC (1,920 ± 151.66 μm, $n = 5$, $p \leq 0.05$) (Fig. 2b).

Although all cell lines successfully integrated in the ventricular wall, they showed a differential pattern of distribution and migration to the lesioned area (Fig. 2b, c–f and d1–f1). In particular, hNSC migrated from the dorsal to the ventral and medio-lateral SVZ and partially to the cc, showing a striking tropism for both the niche (Fig. 2d, d1) and for the lesioned area, whereas T-IhNSC appeared as mostly migrating from the dorsal SVZ to the cc (Fig. 2e, e1) (1.45 mm maximum medio-lateral migration from the injection site, $n = 2$, $p \leq 0.01$). Conversely, v-IhNSC appeared aggregated in small clusters protruding from the ependymal layer (EL) into the ventricular lumen (VL) (Fig. 2f, f1). These results suggested that different hNSC lines display in vivo a common bias to homing, but a specific integration and migration abilities. Interestingly, when we evaluated the presence of astrogliosis in proximity to the SVZ by the expression of GFAP, the immunolabeled area appeared dramatically reduced in transplanted animals (Fig. 2d1–f1) with respect to control lesioned animals (Fig. 2c1). To note, no significant differences were detected in the integration of hNSC-, v-IhNSC-, and

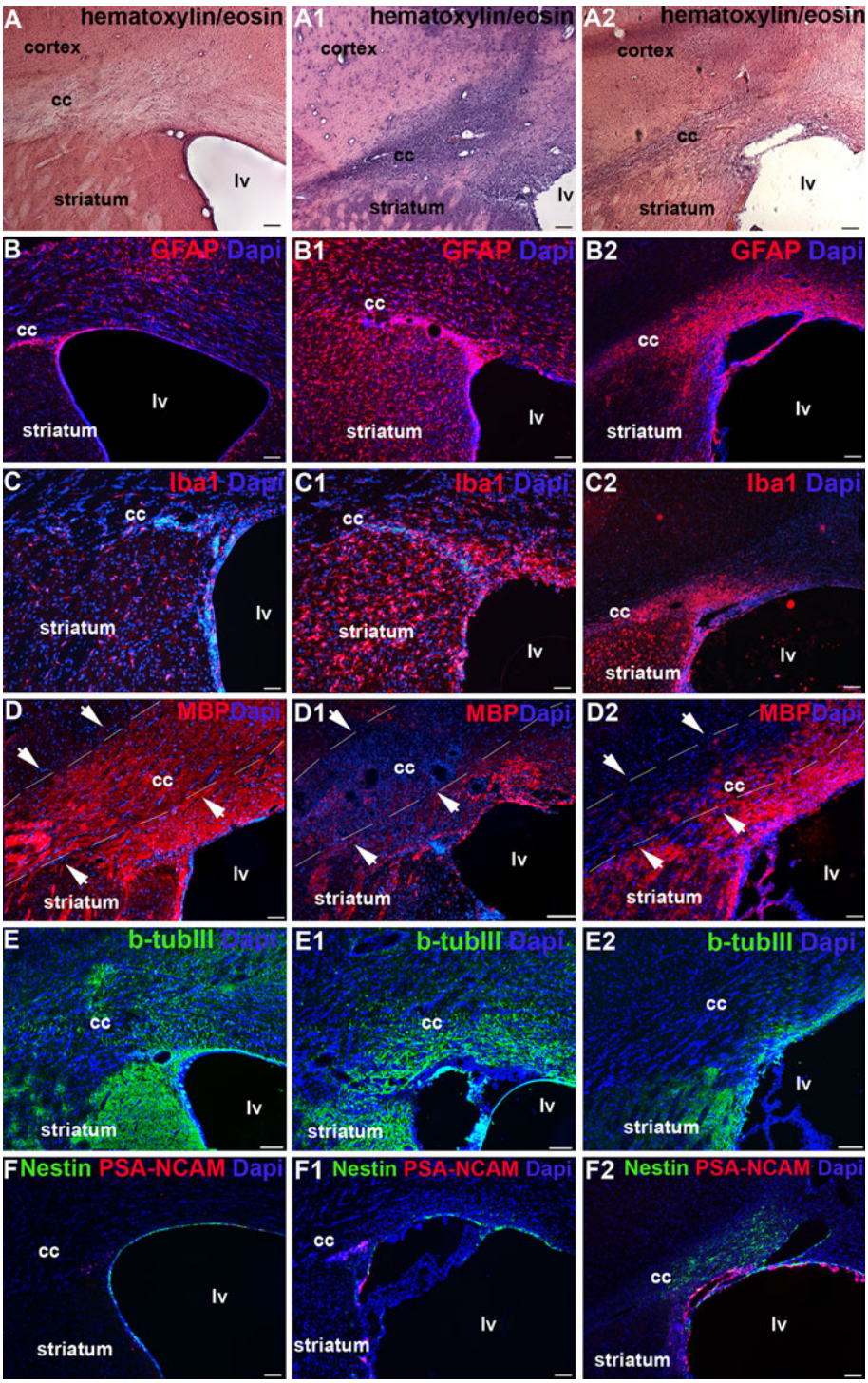


**Fig. 1** Inflammatory reaction and tissue damage after LPC lesion: Analysis of cc in control (not lesioned) rats (**a**–**f**), and animals lesioned at 5 (**a1**–**f1**) and 20 (**a2**–**f2**) days after LPC injection. Immunohistochemistry: **a**–**a2** hematoxylin and eosin; **b**–**b2** GFAP; **c**–**c2** Iba1; **d**–**d2** MBP; **e**–**e2** $\beta$-TubIII; **f**–**f1** nestin/PSA-NCAM. Total nuclei are shown by DAPI staining (*blue*). *Scale bars*, in **a**–**f2** 50 μm. *lv* Lateral ventricle, *cc* corpus callosum

T-IhNSC-derived neural progenitors when transplanted in healthy rats: all the cell lines were detected only in proximity to the injection site, displaying a comparable expression of early markers such as nestin and GFAP. In considering that no distinctive results were obtained in healthy animals, the data presented below refer to lesioned ones. This analysis demonstrates that either immortalized or non-immortalized hNSCs efficiently survive in vivo and their engraftment and migration capacities are differentially improved in lesioned brain.

Among the possible mechanisms responsible for the differential migration to the demyelinated area, we investigated the expression of selected markers involved in the residence of NSC or mobilization of neural progenitors from the SVZ niche. We performed a Western-blot analysis of hNSC-, TIhNSC-, and vIhNSC-derived progenitors

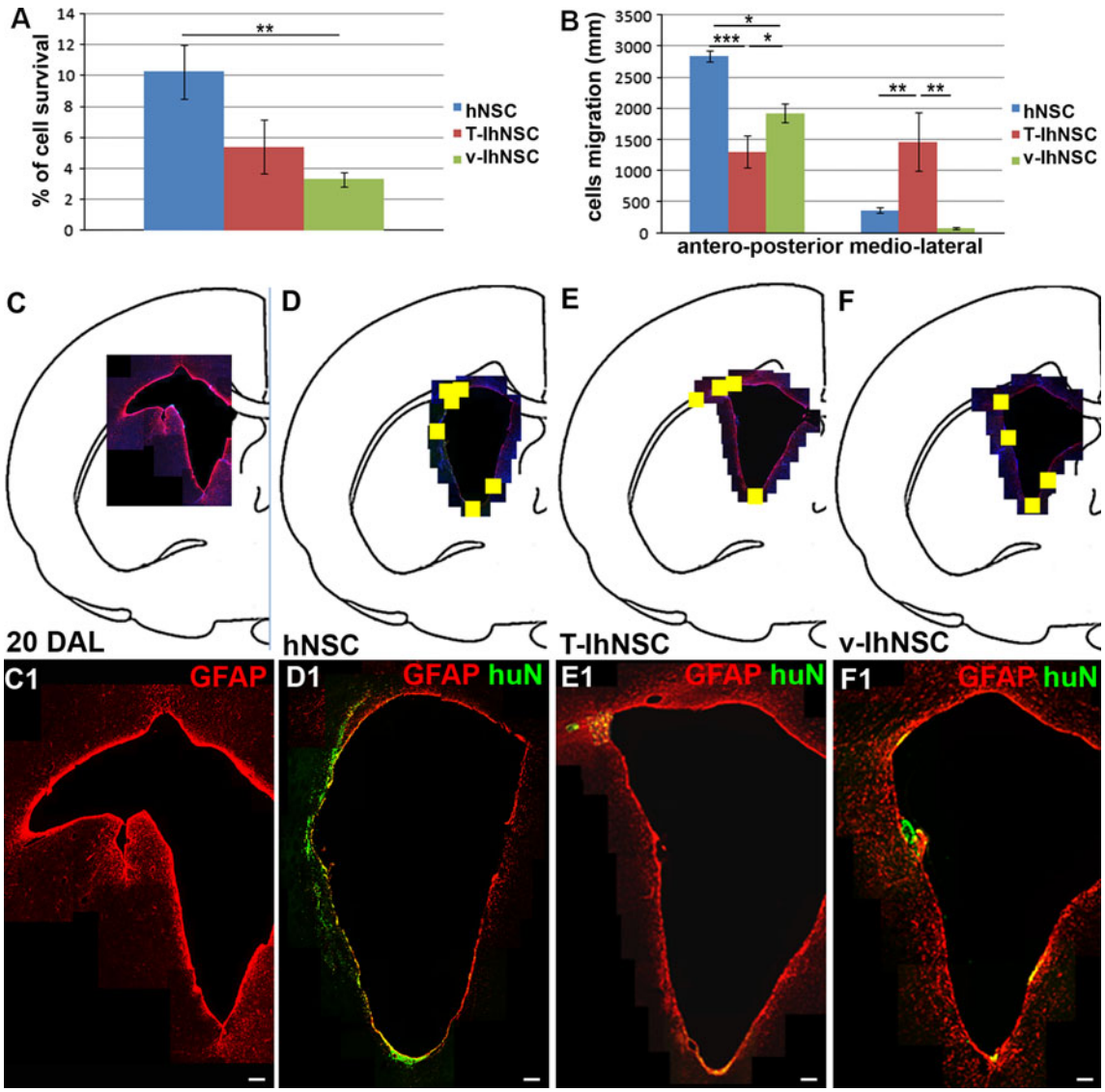


**Fig. 2** Differential distribution of hNSC, T-IhNSC and v-IhNSC into the LPC-lesioned rat brain: quantification of the survival (**a**) and migration ability (**b**) of hNSC and IhNSC. **c–f** Maps showing the activated regions of the SVZ (20 DAL, GFAP+) (**c**, **c1**), colonized (*yellow square*) by transplanted hNSC (**d**), T-IhNSC (**e**), and v-IhNSC (**f**), and respective distribution of huN+ and/or GFAP+ cells in the SVZ (hNSC in **d1**, T-IhNSC in **e1**, and v-IhNSC in **f1**). *Scale bars* in **c1–f1** 50 μm

before transplantation, and a confocal microscopy analysis of the cc and the SVZ 15 days after transplantation. Western-blot analysis showed that in vitro the three lines expressed comparable levels of hSox2, a marker of neural precursor cells, while v-IhNSC displayed a higher expression of notch1, a marker of resident NSC, with respect to T-IhNSC ($p \leq 0.05$) and to hNSC ($p \leq 0.01$) (Fig. 3a, b). A consistent trend was observed in vivo: the three lines generated comparable fractions of hSox2+ (not shown) cells in the SVZ (average 19.83 ± 2.27%, 18.4 ± 1.79%, and 22.76 ± 6.38% of HuN+ cells, respectively, in hNSC, T-IhNSC, and v-IhNSC, $p \geq 0.05$). In contrast, a higher percentage of huN+/notch1+ cells was detectable in rats transplanted with v-IhNSC compared to those transplanted with hNSC and T-IhNSC (respectively, 42 ± 3.2 vs. 37.8 ± 3.5% and 30.4 ± 2.1%, $p \leq 0.05$ Fig. 3c1), in accordance with a major tendency of v-IhNSC to remain in the SVZ (Fig. 2b, 2f, f1). Since previous studies had shown an involvement of CXCL12, EGF, and PDGF in the proliferation and migration of oligodendroglial progenitors toward demyelinated areas [39–45], we investigated their possible relevance in our system. Confocal analysis revealed an enhanced expression of the CXCL12 ligand in the ipsilateral SVZ (Suppl. Fig. 1 a, b) but not in the lesion site or in the contralateral hemisphere (Suppl. Fig. 1b). Consistently, the endogenous expression of CXCR4 and

CXCR7 receptors appeared mostly concentrated in the SVZ (Fig. 3c3–c6). In transplanted animals, in accordance with a comparable expression in vitro (Fig. 3a, b), only sporadic huN+/CXCR4+ and huN+/CXCR7+ cells were detectable (Fig. 3c4, c6) for all the three cell lines.

Similarly, confocal analysis revealed a remarkably higher level of EGF in the SVZ of the ipsilateral hemisphere (Suppl. Fig 1c), with respect to the contralateral one (Suppl. Fig 1d), but only a sporadic and faint EGFR or pEGFR (phosphorylated EGFR, activated form) expression both in resident (Fig. 3c7, c8) and transplanted cells (not shown). These results suggested that neither CXCL12 nor EGF were feasible candidates for the attraction of oligodendroglial progenitors to the lesioned site. We finally analyzed the expression of PDGF (Fig. 3d1, d2) and of its receptors PDGFαR and PDGFβR (Fig. 3d3, d4). The expression of endogenous PDGF appeared to follow a gradient particularly higher in the lesioned cc (Fig. 3d1, d2) compared to the contralateral hemisphere. This pattern was mirrored by a remarkable overexpression of PDGFαR and, while no significant endogenous expression of PDGFβR was detectable, PDGFαR+ progenitors apparently migrating from the SVZ to the cc were evident (white arrow Fig. 3d3). In order to exclude that a transient upregulation of EGF and CXCL12 within few days from LPC injection could account for the induction of transplanted cells to migrate to the lesion, we evaluated the distribution of the ligands at 5 days after LPC injection: the pattern appeared quite similar to that revealed at 15 days, showing that specific upregulation of PDGF expression in the cc appears early after lesion. (not shown).

Interestingly, T-IhNSC and v-IhNSC progenitors displayed in vitro a strikingly higher expression of PDGFαR compared to hNSC (Fig. 3a, b), but this pattern appeared remodeled in vivo. Comparable fractions of hNSC, T-IhNSC, and v-IhNSC were PDGFαR+ in the SVZ (respectively, 31.26 ± 1.16%, 32.21 ± 1.93% and 25.27 ± 4.26% of HuN+ cells, $p \geq 0.05$, Fig. 3d5–d6) but, conversely to CXCR4 and EGFR, PDGFαR expression was retained by both hNSC and T-IhNSC when engrafted in the cc (Fig. 3d7–d8), thus suggesting PDGF as a conceivable candidate for the differential tropism of hNSC and T-IhNSC to the demyelinated areas.

## Analysis of the phenotype of transplanted hNSC lines

The findings above prompted us to investigate the differentiation potentials of the different cell lines. Given the common homing of hNSC, T-IhNSC, and v-IhNSC lines to the SVZ (Fig. 2d–f, d1–f1 and Fig. 4a–c), we first investigated the expression of stemness-related markers like GFAP and nestin by immunofluorescence and confocal microscopy. In the SVZ (Fig. 4d–f), T-IhNSC line generated a significantly lower amount of GFAP+/huN+ cells (30.2 ± 1.5% over total huN+ cells; Fig. 4d–i, p) with respect to hNSC ($p \leq 0.01$) and v-IhNSC ($p \leq 0.001$) which generated, respectively, 43.7 ± 2.8 and 46.6 ± 3.7% of GFAP+ cells. Interestingly, also in the cc T-IhNSC originated a significantly lower number of huN+/GFAP+ cells compared to hNSC (33.7 ± 2.9 vs. 45.01 ± 2.3%, $p \leq 0.05$; Fig. 4p). Most of the cells in the SVZ displayed a globular morphology typical of the resident stem cells (Fig. 4g–i); conversely, GFAP+ cells in the cc appeared star-shaped, consistent with an astroglial phenotype (inset in Fig. 4h).

In parallel, we evaluated the expression of nestin protein. Most of the hNSC and v-IhNSC expressed nestin when integrated in the SVZ (Fig. 4j, l), respectively, 70.2 ± 1.6% and 81.3 ± 1.5% huNestin+/huN+ cells were detected over total huN+ cells (Fig. 4p). As expected [46], these cells were mostly coimmunolabeled by nestin and GFAP markers (Suppl. Fig. 2). By contrast, only 45.4 ± 1.8% of T-IhNSC integrated in the SVZ were huNestin+ ($p \leq 0.01$) (Fig. 4k, 4 p). Interestingly, in the cc, 64.1 ± 1.8% of integrated hNSC and 34.5 ± 1.8% of T-IhNSC were detected as huNestin+ (Fig. 4p), suggesting that the latter have a higher propensity to differentiate.

In order to determine the fraction of proliferating progenitors in situ, we performed immunostaining for the human proliferation marker Ki67. As expected for a population intended to contain migrating progenitors, we observed that only low percentages of hNSC and T-IhNSC were huN+/Ki67+ in the SVZ (Fig. 4m–n) or in the cc (respectively, 7.8 ± 0.5 and 14.3 ± 1.7% in the SVZ and 10.4 ± 1.4 and 10.6 ± 0.6% in the cc), in sharp contrast to v-IhNSC, which were exclusively detected in the SVZ and amounting to 21.6 ± 1.3% huN+/Ki67+ cells ($p \leq 0.01$)

**Fig. 3** Candidate mechanisms for hNSC, T-IhNSC, and v-IhNSC differential migration: Western-blot (**a**) and relative quantification (**b**) of Sox2, notch1, CXCR4, CXCR7, pEGFR, EGFR, PDGFαR, and PDGFβR in hNSC-, T-IhNSC-, and v-IhNSC-derived progenitors. **c** Immunohistochemistry showing the distribution and colocalization with huN+ of putative proteins involved in the integration of transplanted cells into the SVZ. **c1** Chart showing the percentages of huN+/notch1+ cells over total huN+ cells and **c2** confocal image of huN+/notch1+ cells in the ventricular wall. Co-localization of CXCR4 (**c3**, **c4**), CXCR7 (**c5**, **c6**), huEGFR (**c7**), and pEGFR (**c8** and *inset*) with huN+ T-IhNSC in the SVZ. **d** Putative proteins involved in the migration of transplanted cells to the lesioned area. Distribution of endogenous PDGF ligand (**d1–d2**) and PDGFαR (**d3–d4**), respectively, in the lesioned (**d1, d3**) and contralateral (**d2–d4**) hemisphere. Note PDGFR-α+ cells migrating to the lesioned cc (*arrows* **d3**). Co-localization of PDGFαR with huN in lv (**d5, d6**) and in cc (**d7, d8**). Total nuclei are shown by DAPI staining (*blue*). *Scale bars*, in **c1**, **c4** 15 μm, in **c2**, **c7** 23 μm, in **c3**, **c5**, **d1–d5**, **d7** 75 μm, **c6** 7 μm, **c8** 37 μm (*inset* 5 μm) and **d6**, *inset*, **d8** 12 μm. *lv* lateral ventricle and *cc* corpus callosum

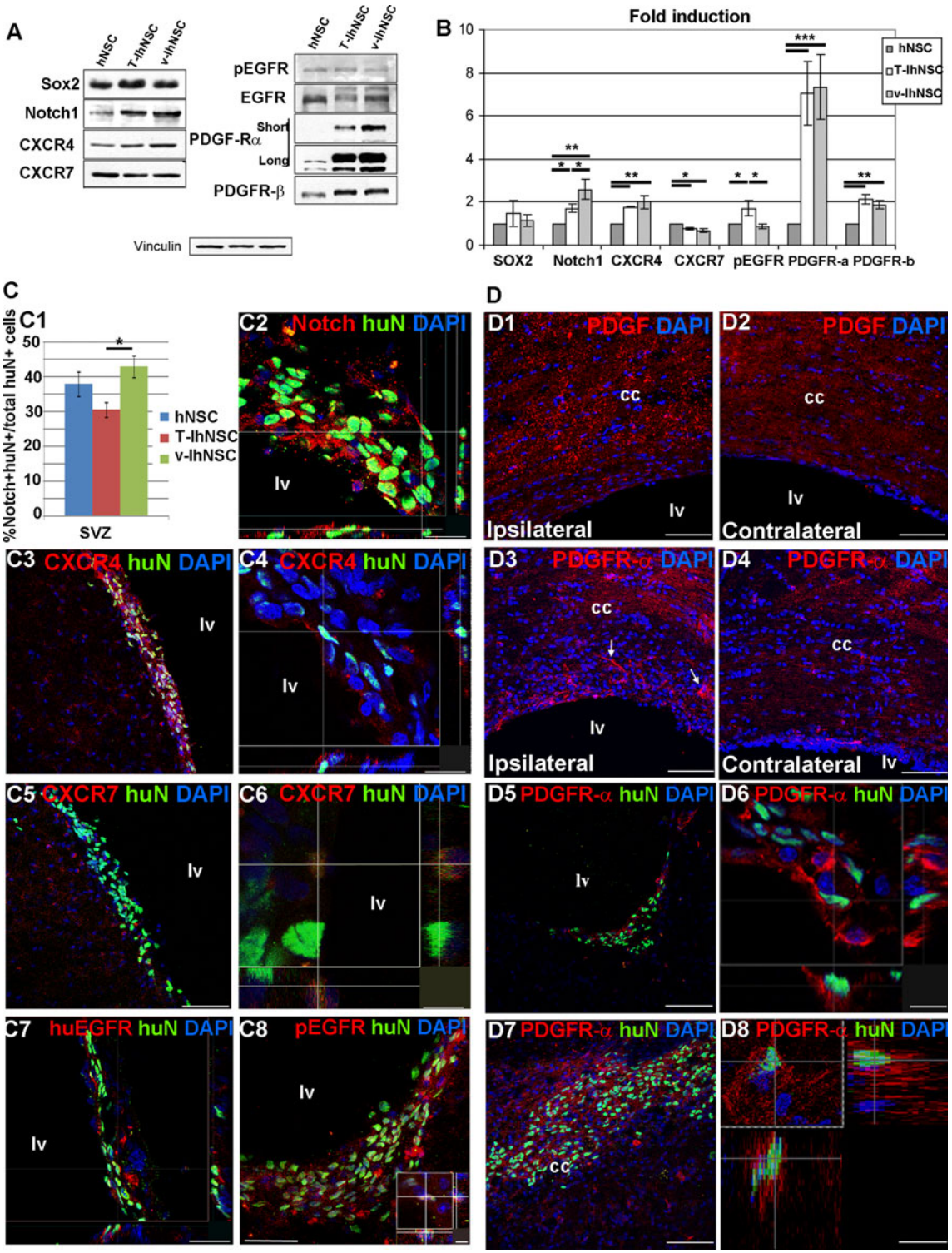


(Fig. 4o–p). These results confirmed that hNSC, T-IhNSC, and v-IhNSC are able to survive after transplantation, to integrate as stem-like cells in the SVZ and to generate dividing progenitors in variable proportions, with T-IhNSC and, even to a lower extent, hNSC rapidly prone to arrest transient proliferation.

## Differentiation and regional specification of hNSC, T-IhNSC, and v-IhNSC to neuronal cells

As previously described, the LPC-induced lesion is spatially confined, transient, and involves mainly the cc, leading also to a progressive neuronal degeneration (Fig. 1e-e2). In view of

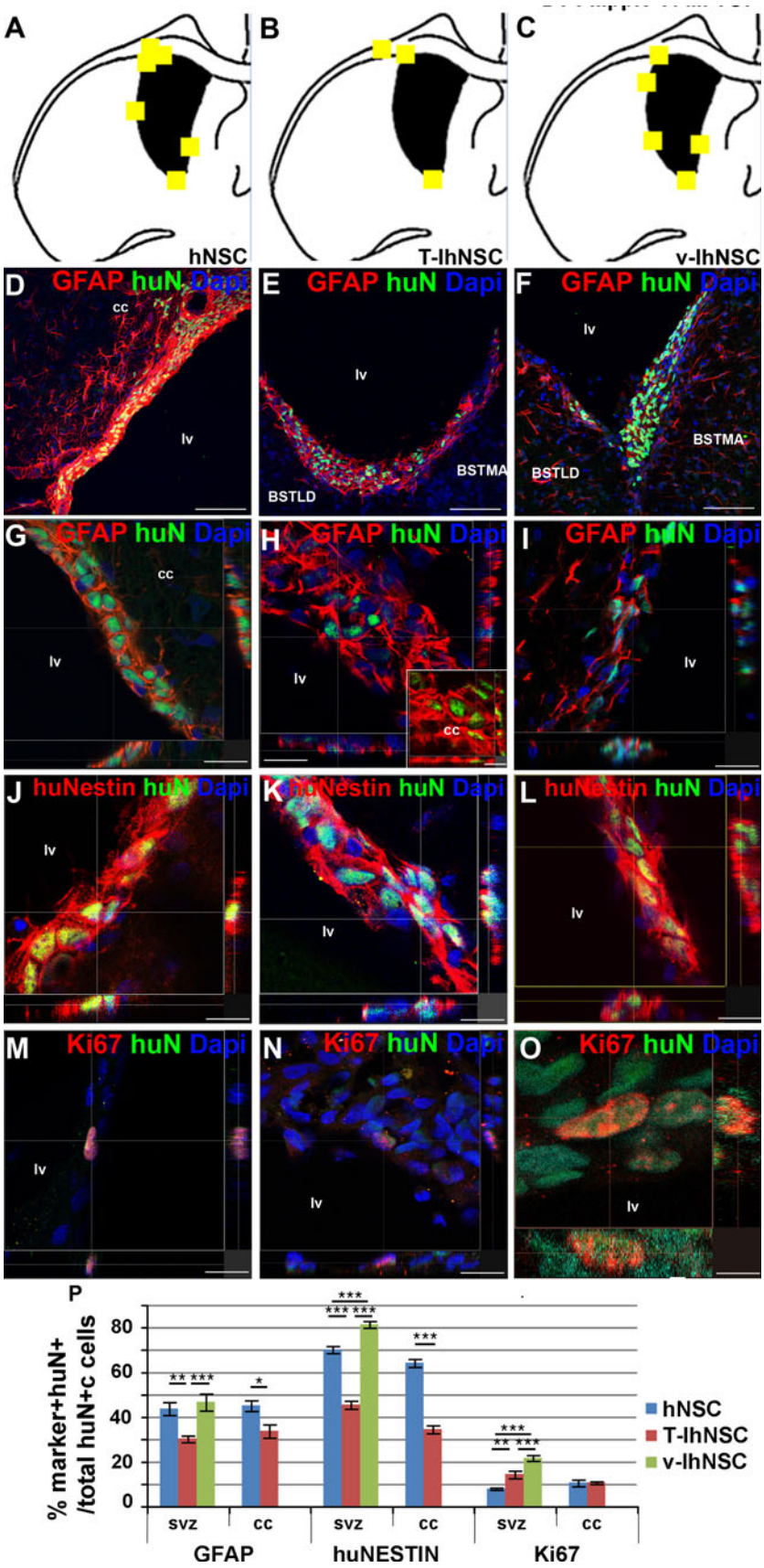


**Fig. 4** Phenotype of transplanted cells into the SVZ (**a–c**) brain map showing the localization of hNSC (**a**), T-IhNSC (**b**), and v-IhNSC (**c**) immunoreactive for GFAP, Nestin, and Ki67 in the SVZ of transplanted rats. **d–i** huN+/GFAP+ cells in rats transplanted with hNSC (**d**, confocal magnification **g**), T-IhNSC (**e**, confocal magnification **h**) and v-IhNSC (**f**, confocal magnification **i**). **j–l** huN+/huNestin+ cells in rats transplanted with hNSC (**j**), T-IhNSC (**k**), and v-IhNSC (**l**). huN+/Ki67+ cells (hNSC M, T-IhNSC N, and v-IhNSC O). Total nuclei are shown by DAPI staining (*blue*). **p** Chart showing the quantification of GFAP+, huNestin+, Ki67+ cells over total huN+ nuclei. *Scale bars*, in **d–f** 75 μm, in **g**, **m**, **i** 19 μm, in **h**, **j**, **k**, **l**, **n** 15 μm (*inset* 10 μm) and in **o** 4 μm. BSTMA and BSTLD, respectively, medial and lateral nucleus of stria terminalis. *lv* lateral ventricle and *cc* corpus callosum

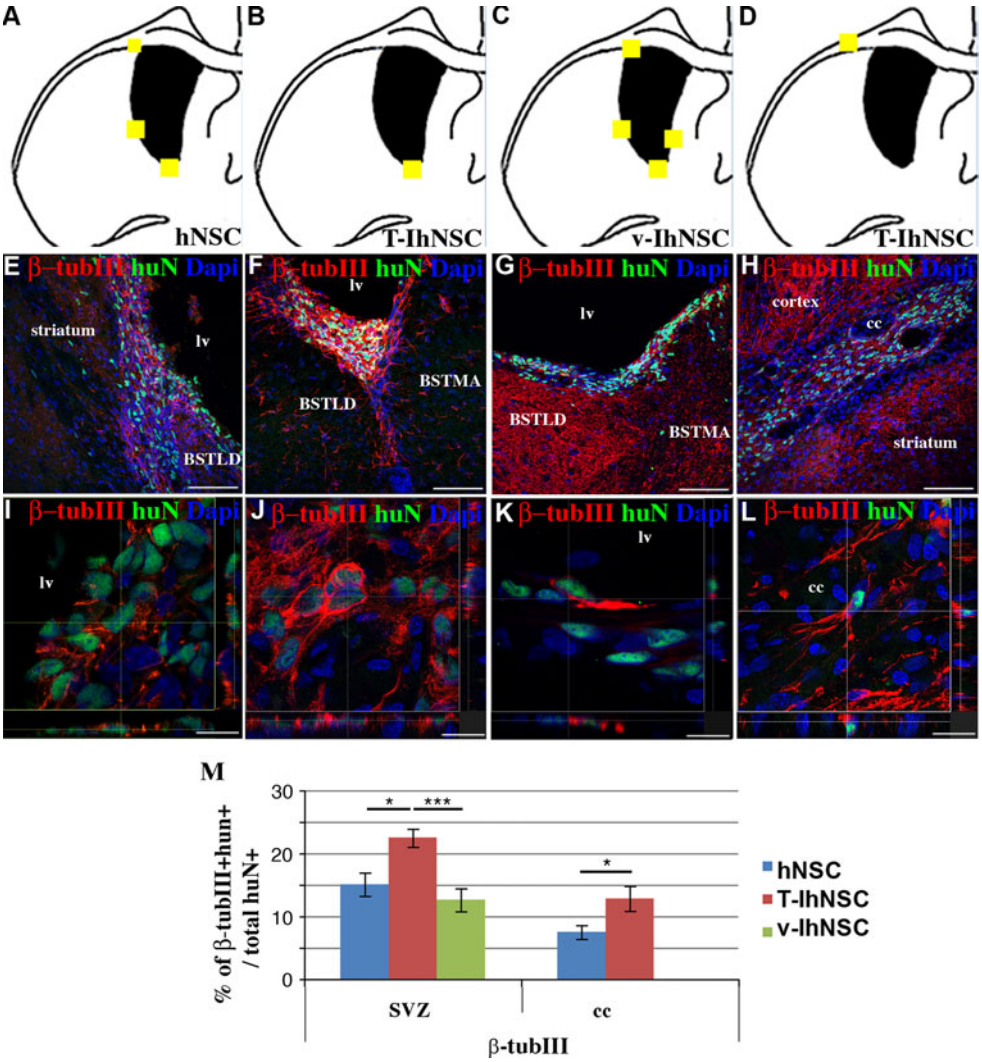


**Fig. 5** Neurons derived from transplanted cells (**a–d**) brain map showing the localization huN+/β-TubIII+ cells for hNSC (**a**), T-IhNSC (**b**, **d**) and v-IhNSC (**c**). **e–h** Distribution of huN+/β-TubIII+ cells into the striatum and SVZ (hNSC in **e**) or along the SVZ wall (T-IhNSC in **f** and v-IhNSC in **g**) or into the cc (T-hNSC in **h**) **i–l** confocal microscopy of huN+/β-TubIII in hNSC (**i**), T-IhNSC (**j**, **l**) and v-IhNSC (**k**). Total nuclei are shown by DAPI staining (*blue*). **m** Quantifications of β-TubIII+ cells over total nuclei. BSTMA and BSTLD, respectively, medial and lateral nucleus of stria terminalis, *lv* lateral ventricle and *cc* corpus callosum. *Scale bars*, in **e–h** 75 μm, in **i** 10 μm, in **j** 16.5 μm, in **k**, **l** 13 μm

the different ability of hNSC, v-IhNSC, and T-IhNSC to integrate in the SVZ and to reach the cc (Fig. 5a–d), we analyzed their propensity to generate β-tubIII+ cells. In the SVZ, all three cell lines gave rise to huN+/β-tubIII+ cells (Fig. 5e–g), with a unipolar morphology (Fig. 5i–k) resembling early neuronal progenitors. Conversely, in the cc, hNSC- and T-IhNSC-derived neuronal progenitors (Fig. 5h) displayed a branching multipolar morphology (Fig. 5l) typical of endogenous resident interneurons. Quantitatively, in the SVZ 15.1 ± 1.9, 22.5 ± 1.4 and 12.6 ± 1.8% of the huN+ cells deriving, respectively, from hNSC, T-IhNSC, and v-IhNSC were β-tubIII+. In the cc, 7.5 ± 1.1% of hNSC and 12.8 ± 2% of T-IhNSC were detected as huN+/β-tubIII+ cells (Fig. 5m). These results suggest that transplanted hNSC, T-IhNSC, and v-IhNSC can give rise to neuronal progenitors in vivo that remain basically immature in the SVZ, while able to migrate and differentiate into the lesioned area. In particular, T-IhNSC displayed a major bias to neuronal cell fate commitment with respect to v-IhNSC ($p \leq 0.001$), which showed a major resilience to early differentiation.

## hNSC and T-IhNSC boost endogenous remyelination and generate oligodendrocytes after migration to the lesioned area

As shown in Fig. 1, the LPC-induced lesion in the cc of the ipsilateral hemisphere is strongly enhanced at 20 DAL with respect to the contralateral hemisphere together with a concomitant mobilization of endogenous stem cells from the SVZ (Fig. 1f1, f2). In order to investigate the different contributions of hNSC and IhNSC to the lesion repair and myelin regeneration, we first evaluated their commitment towards the oligodendroglial phenotype by immunohistochemical analysis of Ng2, a marker of oligodendroglial progenitors (OPC) migrating from the SVZ to the myelinating areas [47]. In the SVZ, a consistent number of huN+/Ng2+ cells were derived from hNSC (20.5 ± 1.4%), T-IhNSC (30.3 ± 1.8%), and v-IhNSC (27.3 ± 1.5%), the latter clustered next to the SVZ (Fig. 6d, g). Interestingly, comparable amounts of Ng2+ progenitors (22.3 ± 1.1% vs. 25.1 ± 1.7%, respectively) deriving from hNSC and

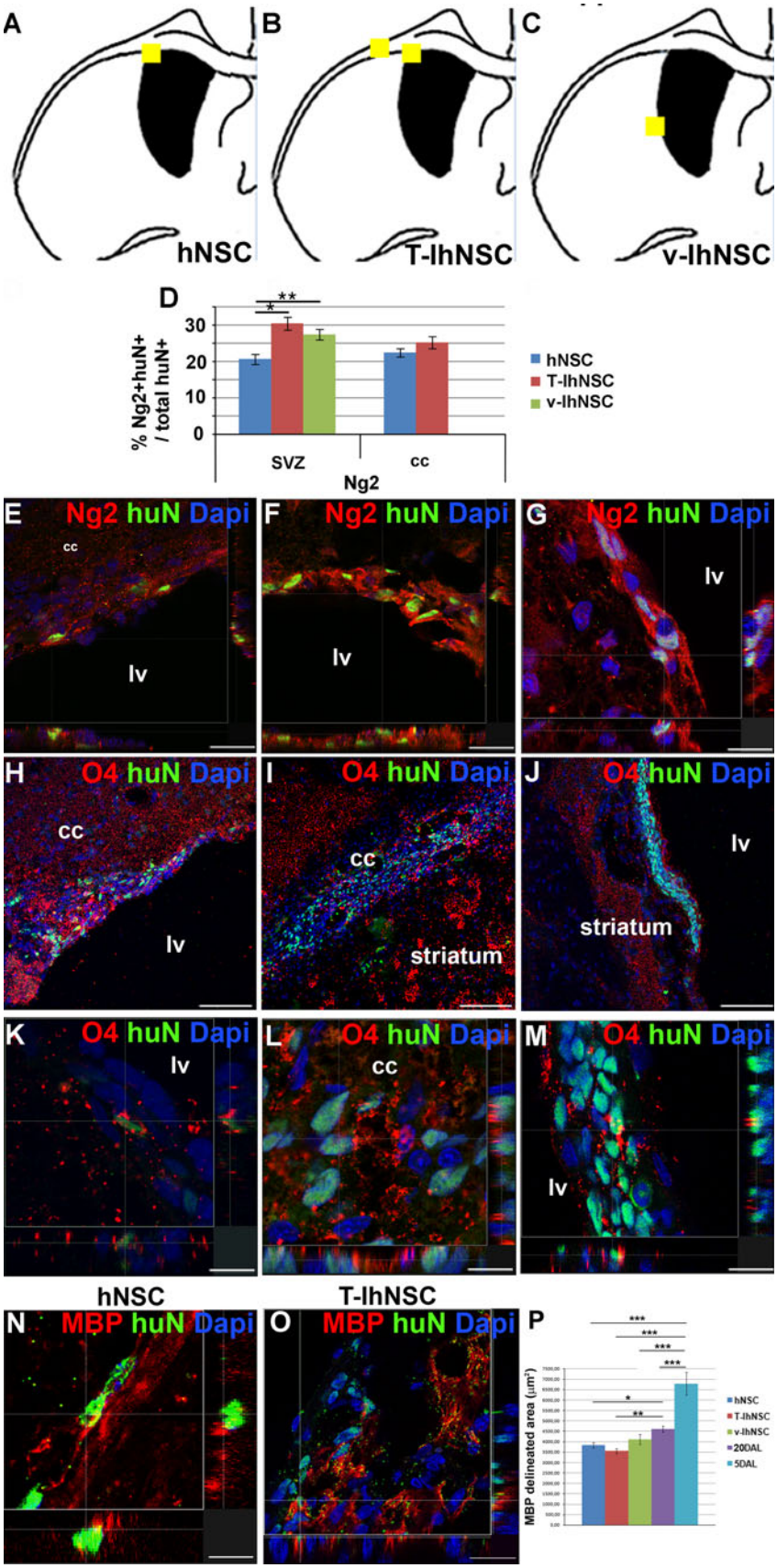


**Fig. 6** Oligodendrocytes derived from transplanted cells (**a–c**) brain map showing the localization of huN+ cells co-expressing oligodendrocyte markers Ng2 O4 and/or MBP: hNSC (**a**), T-IhNSC (**b**), and v-IhNSC (**c**). **d** Quantification of Ng2+ over total huN+ cells. **e–g** Confocal analysis showing huN+/Ng2+: hNSC (**e**), T-IhNSC (**f**), and v-IhNSC (**g**). **h–j** huN+/O4+ cells into the cc (hNSC in **h**; T-IhNSC in **i**, and their, respectively, confocal magnification in **k, l**) and into the striatum close to the ventricular wall (v-IhNSC in **j**, and **m** confocal magnification). **n–o** Confocal analysis of huN+/MBP+ cells in cc deriving from hNSC (**n**) and T-IhNSC (**o**) at 20 DAL. Total nuclei are shown by DAPI staining (*blue*). *Scale bars*, in **e**, **f** 22 µm, in **h–j** 75 µm, in **g**, **k**, **l**, **m** 11 µm, in **o** 20 µm and in **q** 12 µm. *lv* Lateral ventricle and *cc* corpus callosum. **p** Quantification of MBP delineated lesioned area in transplanted and non-transplanted animals ($n = 3$ per condition)

T-IhNSC were detected also in the cc (Fig. 6d). Next, we investigated the expression of the ganglioside O4, a marker of unipotent oligodendroglial progenitors (Fig. 6h–m). Confocal microscopy showed that hNSC ($n = 5/8$) and T-IhNSC ($n = 3/5$) were able to generate O4+ oligodendrocytes (less than 2%) in the cc (Fig. 6a, b), mostly in the demyelinated areas (Fig. 6h–i and k–l). Conversely, v-IhNSC generated only sporadic O4+ cells (Fig. 6j, m) within small clusters of cells proximal to the striatum. Several previous studies showed the capacity of transplanted hNSC to generate oligodendroglial progenitors, but only rarely mature oligodendrocytes [48, 49]. To challenge this limit, we evaluated the expression of the late oligodendroglial markers myelin basic protein (MBP) and quite surprisingly as early as 15 days post-transplant, although occasional, huN+/MBP+ cells were detectable in the lesioned area of hNSC (Fig. 6n, p) and T-IhNSC (Fig. 6o, q) transplanted rats. Most importantly, to determine the effect of the various treatments on the size of the injury site, we stained serial longitudinal sections of the brain (at least three sections per brain, $n = 3$ brains per condition) with anti-MBP antibody. The part marked by high-density MBP-labeling defined the margin of the lesion site, and we measured the unstained (lesioned) area that was surrounded by the dense MBP staining at 5 DAL (6,790.03 ± 546.2 $\mu m^2$). As early as 15 days after, the lesion appeared spontaneously reduced by about 30% (4,606.2 ± 149.8 $\mu m^2$, $p \leq 0.001$). However, following transplantation of IhNSC and hNSC, the lesion was significantly smaller on average, in rats treated with T-IhNSC (3,552.0 ± 117 $\mu m^2$, $p \leq 0.01$) or with hNSC (3,836.8 ± 133.1 $\mu m^2$, $p \leq 0.05$) than in v-IhNSC (4,109.5 ± 239.7 $\mu m^2$, $p \geq 0.05$) or in non-transplanted controls (Fig. 6p). A consistent pattern was observed by measurement of corresponding O4-delineated areas (not shown), suggesting that both early and late re-myelination are facilitated by transplanted cells. Altogether, these results demonstrate that hNSC and T-IhNSC rapidly migrate through the demyelinated areas where they generate oligodendroglial cells and, notably, boost endogenous remyelination, whereas v-IhNSC originate oligodendroglial progenitors with lower propensity to early migration and differentiation.

## Transplanted NSC influence microglia activation

A notable hallmark during the acute phase of the demyelination process is the activation of an inflammatory reaction leading to the development of microgliosis and astrogliosis [36–38, 50]. Thus, we investigated whether the observed differences in the extent of recovery could be correlated with local immunological changes beyond those shown to occur after lesion alone, depending on the contribution of transplanted hNSC to the antiinflammatory component of the endogenous recovery process. To this aim, we analyzed the percentage of Iba1+ microglia in the lesioned hemispheres at 20 DAL (Fig. 7a, b). As suggested from their widespread pattern of migration and rate of survival (Fig. 2a, b), a significant decrease of Iba1+ cells appeared in hNSC-transplanted animals both over antero-posterior and medio-lateral distances with respect to control animals (respectively, $p \leq 0.05$ and $p \leq 0.001$) and to T-hNSC (respectively, $p \leq 0.01$ and $p \leq 0.001$) or v-IhNSC (respectively, $p \leq 0.05$ and $p \leq 0.001$), which also displayed a reliable immunomodulatory effect (Fig. 7a–e). Consistently, we observed a phenotypic modification of the microglial cells in close proximity to hNSC or IhNSC, which partially switched from the globular (macrophagic-activated) morphology (Fig. 7f, g white arrow), to the stellate type (Fig. 7g, yellow arrow), typical of resident microglial cells (Fig. 7h). To assess if hNSC and IhNSC could enhance the modification of microglia in the lesioned area, we evaluated Iba1+ cells in different regions such as the corpus callosum adjacent to the rostral migratory stream (cc/RMS), corpus callosum (cc), lateral SVZ (l-SVZ), and ventral SVZ (v-SVZ) where hNSC, v-IhNSC, and T-IhNSC were detected. The rate of reduction of microglia in the lesioned brain areas correlated with the distribution of the engrafted cells (Fig. 7a): it was maximal in the cc/RMS where hNSC appeared as the most effective cells leading to a reduction of Iba1+ cells from 55.4 ± 1.5% (lesioned control) to 23.6 ± 2.1% ($p \leq 0.001$), compared with a reduction to 37.1 ± 3.1% by v-IhNSC ($p \leq 0.01$) and to 36.7 ± 3.7% by T-IhNSC ($p \leq 0.01$) (Fig. 7i). The effect was still evident in the cc where hNSC and T-IhNSC were comparably able to decrease Iba1+ cells from 61.1 ± 7.3% in control animals to 30.9 ± 5.5% ($p \leq 0.05$) and 30.3 ± 2% ($p \leq 0.01$), respectively, and v-IhNSC to 42.8 ± 6.7% (Fig. 7i). No significant change of microglial cells was observed in the lateral or ventral SVZ (Fig. 7i), which were not affected by the lesion. Since Iba1 labels both resident and activated microglial cells, we investigated the specific NSC-mediated dampening of reactive CD68+ cells in the cc-SVZ area where peaked the inflammatory reaction. Following the lesion, at 5 DAL, a significant percentage (25.5 ± 3.3%) of CD68+ cells were evident in the lesion site (cc-SVZ) (Fig. 7j, k), but not in the contralateral hemisphere. At 20 DAL, the number of CD68+ cells was spontaneously reduced to 20.2 ± 1.37% (Fig. 7j, l) in non-transplanted animals, but it appeared dramatically down-modulated in transplanted animals, with hNSC exerting the highest effect (8.94 ± 1.1%, $p \leq 0.001$) (Fig. 7j, m) and T-IhNSC to a similar, although lower, extent (12.47 ± 1.0%, $p \leq 0.05$) (Fig. 7j, n). A similar trend was observed in v-IhNSC transplanted animals, but the reduction was not statistically significant (15.86 ± 1.2%, $p \geq 0.05$)

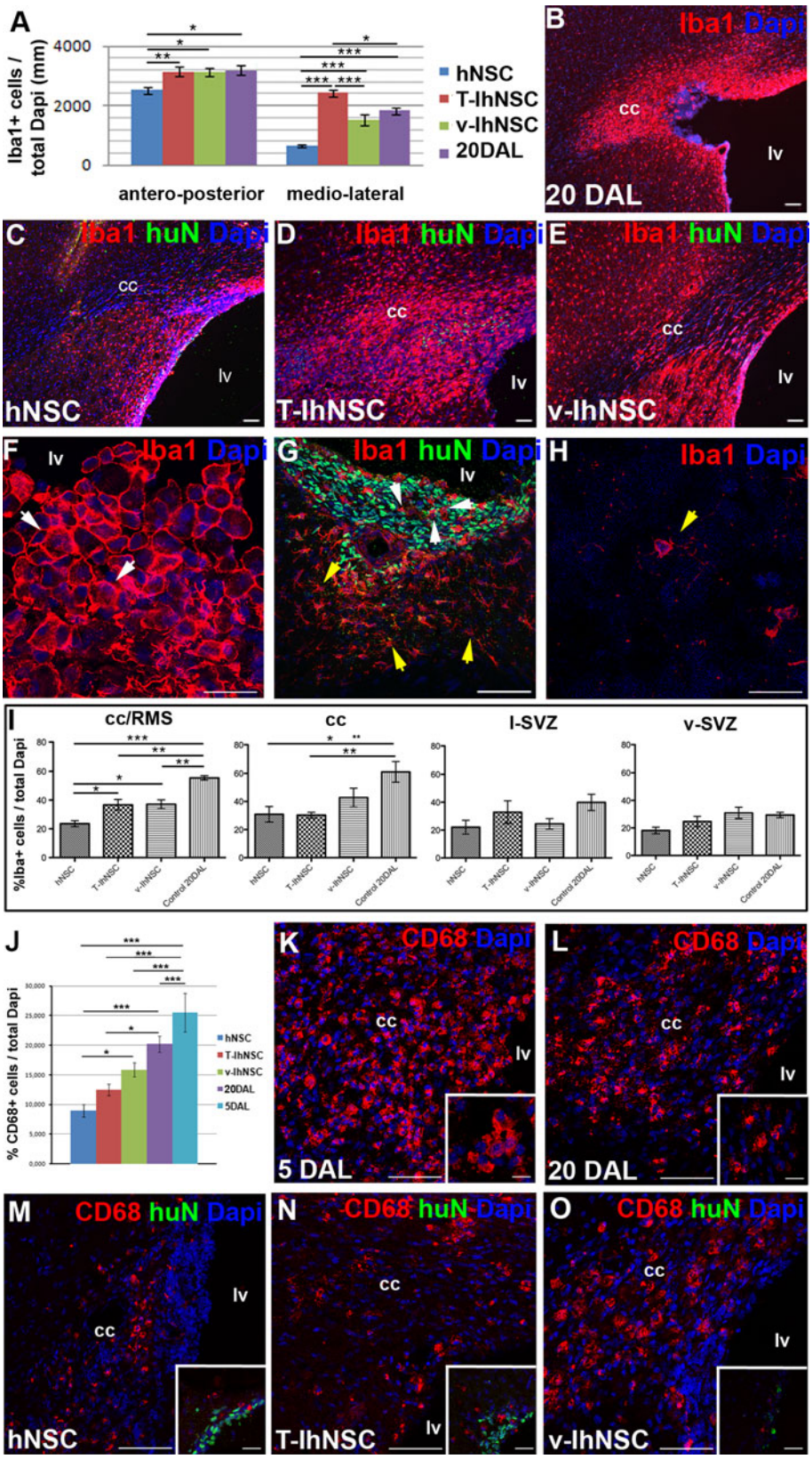


**Fig. 7** Evaluation of activated microglia (**a**) quantification of the activated microglia extension into the cc of lesioned and transplanted rats. **b–e** Representative images showing the diverse distribution of activated microglia (Iba1+) in lesioned control rats at 20 DAL (**b**) or in lesioned animals transplanted with hNSC (**c**, huN+), T-IhNSC (**d**, huN+) or v-IhNSC (**e**, huN+). **f–h** Microglial morphology in lesioned (**f**) and transplanted (**g**) and non-lesioned animals (**h**). Total nuclei are shown by DAPI staining (*blue*). **i** Quantification of Iba1+ cells in cc/RMS, cc lateral sub-ventricular zone l-SVZ, ventral sub-ventricular zone (v-SVZ). **j** Quantification of CD68+ (*red*) cells in the cc/RMS of lesioned and transplanted rats. **k–o** Representative images showing the diverse distribution of activated microglia (CD68+) in lesioned control rats at 5 DAL (**k**), 20 DAL (**l**), or in lesioned animals transplanted with hNSC (**m**, *inset* huN+ *green*), T-IhNSC (**n**, huN+ *green*) or v-IhNSC (**o**, huN+ *green*). *Scale bars*, in **b–e** 50 μm, **k–o** 60 μm, in **f–h** 21 μm and in **g** 75 μm, *inset* **k** 10 μm, *insets* **l–o** 30 μm

(Fig. 7j, o). These results showed that either hNSC or IhNSC are able to modulate the local inflammatory reaction after injury, with hNSC being more effective than IhNSC.

## Discussion

In this study, we have transplanted non-immortalized hNSC, v-IhNSC, and T-IhNSC progenitors next to the ventricular wall (SVZ) of adult rats injured by lysophosphatidylcholine (LPC) to evaluate their integration and maturation in a pathological setting mimicking the acute demyelination. We documented their differential tropism to the lesioned area and their differential abilities to stimulate the endogenous recovery, to spawn oligodendroglial cells, and to modulate the inflammatory environment in the lesion site. It has to be emphasized that, here, we compare for the first time a non-immortalized hNSC line with v-IhNSC and T-IhNSC lines and, in particular, that this is the first study investigating the therapeutic potential of T-IhNSCs in vivo.

A relatively limited number of studies has reported the capacity of transplanted progenitor cells to generate myelin-forming oligodendrocytes in vivo [48, 49].

We injected NSC-derived progenitor cells when, although gliosis and inflammatory reaction are still active [51], transplanted cells can benefit from the environmental cues generated by the initial phase of endogenous remyelination [52] and are not yet suffering from the detrimental effects induced by acute reactive astrogliosis and microgliosis [36–38, 53]. Indeed, although the inflammatory reaction occurring soon after an acute injury is scarcely permissive to the survival of exogenous cells [54, 55], we previously had shown that v-IhNSC and hNSC are able to survive for the long term in adult rat brains lesioned by global ischemia, even under transient immunosuppression [28].

In LPC-lesioned rats, we chose to transplant a mixed population of hNSC- or IhNSC-derived neural progenitors in order to favor their rapid integration and differentiation.

The three lines all successfully engrafted, but, interestingly, they displayed a different pattern of migration to the lesion site and differentiation (pathotropism), although sharing a common tropism to the SVZ niche (homing). At 20 DAL, T-IhNSC showed an enhanced bias to intraparenchymal migration and rapidly followed the route to the demyelinated site, while hNSC appeared only partially targeted to the lesion site and mostly distributed along the ventricular wall. Conversely, v-IhNSC were still approaching a full integration into the SVZ and remained prevalently aggregated in small cell clusters, occasionally protruding into the ventricular lumen (VL). These observations were consistent with previous studies demonstrating that lesioned environment after acute injuries, such as stroke or focal ischemia, exerts an attractive effect on exogenous healthy cells [23, 56]. In order to elucidate which mechanisms could account for the differential pathotropism of hNSC and IhNSC, we investigated the expression of markers involved in the maintenance or mobilization of NSC from the SVZ niche. Consistently with their resilience to early migration in vivo, we observed that v-IhNSC intrinsically displayed an enhanced expression of notch1, which is responsible for keeping NSC in a quiescent state [40], compared to hNSC or to T-IhNSC. On the other hand, although CXCR4 has been shown to be involved in the migration of oligodendroglial progenitors to demyelinated areas following CXCL12 gradient induced by the lesion [42], a significant expression of both CXCL12 and CXCR4 was detectable only in the SVZ. Comparable results were obtained when we analyzed the expression of EGFR and of its activated phosphorylated isoform (pEGFR), known to enhance the remyelination ability of oligodendroglial progenitors from the SVZ after focal demyelination of EGFR mutant mice [39]. To note, similarly to CXCL12, EGF expression appeared enhanced in the ipsilateral hemisphere compared to the contralateral one, suggesting that both CXCL12 and EGF could be more likely involved in the integration of transplanted cells into the SVZ niche than in their targeting to the lesion. These results prompted us to investigate PDGF signaling. Importantly, 30% of the T-IhNSC migrated to cc appeared PDGFαR+, in accordance with the enhanced expression of both the PDGF ligand and the endogenous receptor in the lesioned hemisphere compared to the contralateral one. Recent studies from Kang et al. [47] have shown that in the normal as in the lesioned CNS, NG2+ progenitors are specifically recruited and committed to the oligodendroglial lineage, with mostly of them expressing PDGFαR [57]. Since we observed from 20% (hNSC) to 30% (T-IhNSC) of HuN+/NG2+ cells both in the SVZ and in the cc, we hypothesized that a fraction of human NG2+ progenitors could have migrated from the SVZ to the cc. These findings, together with previous studies showing the involvement of PDGF in the recruitment of OPCs to the lesion [41, 43, 44], suggest that NG2+ cells mostly account for the physiological response to demyelination. Most importantly, we showed that, besides their own remyelinating capacity, T-IhNSC and hNSC significantly enhanced endogenous remyelination. The mechanism/s that underpin the remyelination process have still to be elucidated. Here we have shown PDGF as a feasible candidate for the differential pathotropism of hNSC, v-IhNSC, and T-IhNSC. Although beyond the aim of this work, future experiments leading to the overexpression and/or silencing of PDGF ligand or PDGFR directly in vivo would provide further evidence to test our hypothesis. The lack of relevant correlations between the expression patterns displayed by hNSC and IhNSC lines, respectively, in vitro and in vivo,

suggests that multiple non-cell-autonomous mechanisms could be involved in their recruitment to the lesion [40, 58].

## Oligodendrogenic and immunomodulatory effects of hNSC and IhNSC

After LPC-induced lesion, hNSC, T-IhNSC, and v-IhNSC lines were able to contribute to myelin regeneration to a different extent. v-IhNSC were able to generate Ng2+ and only sporadic O4+ progenitors in the SVZ, consistent with their immature phenotype and delayed migration ability, while hNSC and T-IhNSC generated Ng2+ and O4+ precursors in both SVZ and demyelinated cc. At variance with previous studies showing that differentiation of hNSC into mature myelinating oligodendrocytes requires species-specific signals [59, 60] and a long time after transplantation [26, 48, 49, 61, 62], we demonstrate the appearance of isolated hNSC- or T-IhNSC-derived myelinating MBP + oligodendrocytes as early as 15 days following transplantation with a concomitant and enhancement of spontaneous remyelination compared to animals injected with HBSS saline buffer solution. It has to be emphasized that remyelination arose, overall, from endogenous cells, given the negligible colocalization of the oligodendroglial and huN markers, despite the fact that the latter was readily detected all throughout the transplant and neighboring regions. Furthermore, we cannot exclude that v-IhNSC could similarly contribute to myelin regeneration in other animal models with a long-term progression of the demyelination injury.

Most importantly, one of the hallmarks characterizing most demyelinating disorders like multiple sclerosis (MS), spinal cord injury (SCI), amyotrophic lateral sclerosis (ALS), metachromatic leukodystrophy (MLD), lysosomal storage diseases (LSDs) [21, 63], and also neurodegenerative disorders such as Parkinson's disease (PD), Alzheimer's disease (AD), and stroke, is the development of an inflammatory environment, which can contribute to tissue damage or, at least, delay the spontaneous recovery. Recent studies have elucidated that the therapeutic potential of NSCs relies even on their immunomodulatory capacity [28, 64–66]. Our study reports that transplantation of hNSC and IhNSC lines can effectively dampen microglia activation in the injured areas. To note, non-immortalized hNSC were able to induce a significant reduction of activated microglia extension, together with the incipient conversion of the globular-macrophagic into the stellate phenotype, typical of resident microglia. This effect occurred exclusively in the transplanted regions, confirming the existence of differential, locoregional instructive cues in the lesioned site, although this issue would require further studies to be unraveled.

In conclusion, these data demonstrate efficient in vivo survival of both immortalized and non-immortalized hNSCs, region-specific integration, migration to the lesion, oligodendroglial differentiation accompanied by the boosting of endogenous recovery, and immunomodulation of the local inflammatory environment as early as 15 days from transplantation into the focally demyelinated brain of adult rats. In particular, a novel immortalized hNSC line [16], T-IhNSC, has been tested in vivo for the first time, showing a remarkable migration ability and bias to oligodendroglial fate differentiation. We have for the first time compared in vivo non-immortalized hNSC with immortalized akin cells, with non-immortalized hNSC emerging as the most effective to exert immunomodulatory and neuroprotective effects. On the other hand, two different IhNSC lines, differing for the respective expression of two variants of the myc gene, have displayed striking differences either in migration and differentiation capacities, although retaining a basal bias to efficient survival rate and engraftment. It has to be emphasized that either hNSCs or IhNSCs never displayed a tumorigenic potential. Indeed, the immunostaining for the proliferative marker Ki67 showed that a fraction lower than 11% of Ki67+/huN+ cells was detectable in the cc as early as at 15 days after transplantation. Consistently we had previously shown that both hNSC and IhNSC rapidly arrest to proliferate in vivo, since only sporadic Ki67+/huN+ cells could be detectable as early as at 1 month from transplantation in the adult ischemic rat brain [28] and no aberrant proliferation was ever observed up to 6 months from transplantation of hNSC or IhNSC into the striatum of SCID mice (unpublished results, [14]). The availability of large pools of in vitro expanded IhNSCs and GMP grade hNSCs with no ethical concerns offers the possibility to perform further ex vivo manipulations and, most importantly, to obtain different neural phenotypes. If IhNSC represent an inexhaustible source of hNSC available for large-scale preclinical studies, non-immortalized GMP grade hNSC lines can be promoted as an efficacious, safe, and reliable therapeutic source to be harnessed in forthcoming clinical applications. Therefore, the ability to target hNSC fate choice by modulating their intrinsic properties could be pivotal to the employment of hNSC in the therapy of neurodegenerative diseases.

## Conclusions and implications for future NSC-based therapies

In this study, we have transplanted non-immortalized hNSC, v-IhNSC, and T-IhNSC progenitors next to the ventricular wall (SVZ) of adult rats injured by lysophosphatidylcholine (LPC) to evaluate their integration and maturation in a pathological setting mimicking the acute demyelination. We documented their differential ability to engraft efficiently, with a remarkably negligible rejection,

to home to the host niche and to migrate to the lesioned area, where they could boost endogenous repair, differentiate as mature oligodendroglial cells, and modulate the inflammatory environment generated by the lesion.

In conclusion, these results support the use of appropriate IhNSC lines as useful tools for translational studies on demyelinating neuronal disorders and provide a reinforcing element when considering the therapeutic role of hNSC for the cure of neurodegenerative diseases like Alzheimer's disease, Parkinson's disease, Amyotrophic lateral sclerosis, and stroke, characterized by pathological hallmarks such as neurodegeneration, demyelination, and inflammation. This is particularly relevant in view of the parallel establishment of GMP-grade hNSC lines for a phase I clinical trial that is currently underway pointing to different hNSC lines as being reliable sources for addressed NSC-mediated cell therapies of neurodegenerative diseases.

**Acknowledgments** We thank Pietro De Filippis, Patrizia Karoschitz, Cesare Rota Nodari, Loredana Turani, Antonio Tomaino, for precious suggestions. This work was supported by the CARIPLO Foundation; Neurothon ONLUS Foundation; Italian Association for Cancer Research (AIRC); Italian Ministry of Health (Ricerca Finalizzata). This work was financially supported by grants from the CARIPLO Foundation, the Neurothon ONLUS Foundation, Fondazione Borgonovo ONLUS, and by the Italian Association for Cancer Research (AIRC), the Italian Ministry of Health (Ricerca Finalizzata), and Stemgen S.p.a.

## References

1. Alvarez-Buylla A, Garcia-Verdugo JM, Tramontin AD (2001) A unified hypothesis on the lineage of neural stem cells. Nat Rev Neurosci 2(4):287–293
2. Gage FH (2000) Mammalian neural stem cells. Science 287(5457):1433–1438
3. Temple S (2001) The development of neural stem cells. Nature 414(6859):112–117
4. Popa-Wagner A, Buga AM, Kokaia Z (2009) Perturbed cellular response to brain injury during aging. Ageing Res Rev 10(1):71–79
5. Romanko MJ, Rola R, Fike JR, Szele FG, Dizon ML, Felling RJ, Brazel CY, Levison SW (2004) Roles of the mammalian sub-ventricular zone in cell replacement after brain injury. Prog Neurobiol 74(2):77–99
6. Craig CG, Tropepe V, Morshead CM, Reynolds BA, Weiss S, van der Kooy D (1996) In vivo growth factor expansion of endogenous subependymal neural precursor cell populations in the adult mouse brain. J Neurosci 16(8):2649–2658
7. Kuhn HG, Winkler J, Kempermann G, Thal LJ, Gage FH (1997) Epidermal growth factor and fibroblast growth factor-2 have different effects on neural progenitors in the adult rat brain. J Neurosci 17(15):5820–5829
8. Martinez-Serrano A, Fischer W, Bjorklund A (1995) Reversal of age-dependent cognitive impairments and cholinergic neuron atrophy by NGF-secreting neural progenitors grafted to the basal forebrain. Neuron 15(2):473–484
9. Vescovi AL, Gritti A, Galli R, Parati EA (1999) Isolation and intracerebral grafting of nontransformed multipotential embryonic human CNS stem cells. J Neurotrauma 16(8):689–693
10. Vescovi AL, Parati EA, Gritti A, Poulin P, Ferrario M, Wanke E, Frolichsthal-Schoeller P, Cova L, Arcellana-Panlilio M, Colombo A, Galli R (1999) Isolation and cloning of multipotential stem cells from the embryonic human CNS and establishment of transplantable human neural stem cell lines by epigenetic stimulation. Exp Neurol 156(1):71–83
11. Gallo V, Armstrong RC (2008) Myelin repair strategies: a cellular view. Curr Opin Neurol 21(3):278–283
12. Goldman SA (2007) Disease targets and strategies for the therapeutic modulation of endogenous neural stem and progenitor cells. Clin Pharmacol Ther 82(4):453–460
13. Vescovi AL, Reynolds BA, Fraser DD, Weiss S (1993) bFGF regulates the proliferative fate of unipotent (neuronal) and bipotent (neuronal/astroglial) EGF-generated CNS progenitor cells. Neuron 11(5):951–966
14. De Filippis L, Lamorte G, Snyder EY, Malgaroli A, Vescovi AL (2007) A novel immortal and multipotent human neural stem cell line generating functional neurons and oligodendrocytes. Stem Cells 25(9):2312–2321
15. Villa A, Snyder EY, Vescovi A, Martinez-Serrano A (2000) Establishment and properties of a growth factor-dependent perpetual neural stem cell line from the human CNS. Exp Neurol 161(1):67–84
16. De Filippis L, Ferrari D, Rota Nodari L, Amati B, Snyder E, Vescovi AL (2008) Immortalization of human neural stem cells with the c-myc mutant T58A. PLoS One 3(10):e3310
17. Behrstock S, Ebert A, McHugh J, Vosberg S, Moore J, Schneider B, Capowski E, Hei D, Kordower J, Aebischer P, Svendsen CN (2006) Human neural progenitors deliver glial cell line-derived neurotrophic factor to parkinsonian rodents and aged primates. Gene Ther 13(5):379–388
18. Ebert AD, Svendsen CN (2005) A new tool in the battle against Alzheimer's disease and aging: ex vivo gene therapy. Rejuvenation Res 8(3):131–134
19. Lee HJ, Kim KS, Park IH, Kim SU (2007) Human neural stem cells over-expressing VEGF provide neuroprotection, angiogenesis and functional recovery in mouse stroke model. PLoS One 2(1):e156
20. Suzuki M, McHugh J, Tork C, Shelley B, Klein SM, Aebischer P, Svendsen CN (2007) GDNF secreting human neural progenitor cells protect dying motor neurons, but not their projection to muscle, in a rat model of familial ALS. PLoS One 2(1):e689
21. Lindvall O, Kokaia Z (2010) Stem cells in human neurodegenerative disorders–time for clinical translation? J Clin Invest 120(1):29–40
22. Blurton-Jones M, Kitazawa M, Martinez-Coria H, Castello NA, Muller FJ, Loring JF, Yamasaki TR, Poon WW, Green KN, La Ferla FM (2009) Neural stem cells improve cognition via BDNF in a transgenic model of Alzheimer disease. Proc Natl Acad Sci USA 106(32):13594–13599
23. Boockvar JA, Schouten J, Royo N, Millard M, Spangler Z, Castelbuono D, Snyder E, O'Rourke D, McIntosh T (2005) Experimental traumatic brain injury modulates the survival, migration, and terminal phenotype of transplanted epidermal growth factor receptor-activated neural stem cells. Neurosurgery 56(1):163–171
24. Englund U, Bjorklund A, Wictorin K (2002) Migration patterns and phenotypic differentiation of long-term expanded human neural progenitor cells after transplantation into the adult rat brain. Brain Res Dev Brain Res 134(1–2):123–141
25. Pluchino S, Gritti A, Blezer E, Amadio S, Brambilla E, Borsellino G, Cossetti C, Del Carro U, Comi G, Hart BT, Vescovi A, Martino G (2009) Human neural stem cells ameliorate autoimmune

encephalomyelitis in non-human primates. Ann Neurol 66(3): 343–354
26. Neri M, Maderna C, Ferrari D, Cavazzin C, Vescovi AL, Gritti A (2010) Robust generation of oligodendrocyte progenitors from human neural stem cells and engraftment in experimental demyelination models in mice. PLoS One 5(4):e10145
27. Pluchino S, Quattrini A, Brambilla E, Gritti A, Salani G, Dina G, Galli R, Del Carro U, Amadio S, Bergami A, Furlan R, Comi G, Vescovi AL, Martino G (2003) Injection of adult neurospheres induces recovery in a chronic model of multiple sclerosis. Nature 422(6933):688–694
28. Rota Nodari L, Ferrari D, Giani F, Bossi M, Rodriguez-Menendez V, Tredici G, Delia D, Vescovi AL, De Filippis L (2010) Long-Term Survival of Human Neural Stem Cells in the Ischemic Rat Brain upon Transient Immunosuppression. PLoS One 5(11):e14035
29. Hall SM (1972) The effect of injections of lysophosphatidyl choline into white matter of the adult mouse spinal cord. J Cell Sci 10(2):535–546
30. Nait-Oumesmar B, Decker L, Lachapelle F, Avellana-Adalid V, Bachelin C, Van Evercooren AB (1999) Progenitor cells of the adult mouse sub-ventricular zone proliferate, migrate and differentiate into oligodendrocytes after demyelination. Eur J Neurosci 11(12):4357–4366
31. Taupin P (2006) HuCNS-SC (stem cells). Curr Opin Mol Ther 8(2):156–163
32. Raore B, Federici T, Taub J, Wu MC, Riley J, Franz CK, Kliem MA, Snyder B, Feldman EL, Johe K, Boulis NM (2011) Cervical multilevel intraspinal stem cell therapy: assessment of surgical risks in Göttingen mini pigs. Spine 36(3):E164–E171
33. Stroemer P, Patel S, Hope A, Oliveira C, Pollock K, Sinden J (2009) The neural stem cell line CTX0E03 promotes behavioral recovery and endogenous neurogenesis after experimental stroke in a dose-dependent fashion. Neurorehabil Neural Repair 23(9):895–909
34. Carlessi L, De Filippis L, Lecis D, Vescovi A, Delia D (2009) DNA-damage response, survival and differentiation in vitro of a human neural stem cell line in relation to ATM expression. Cell Death Differ 16(6):795–806
35. Abercrombie M (1946) Estimation of nuclear population from microtome sections. Anat Rec 94:239–247
36. Ghasemlou N, Jeong SY, Lacroix S, David S (2007) T cells contribute to lysophosphatidylcholine-induced macrophage activation and demyelination in the CNS. Glia 55(3):294–302
37. Ousman SS, David S (2000) Lysophosphatidylcholine induces rapid recruitment and activation of macrophages in the adult mouse spinal cord. Glia 30(1):92–104
38. Ousman SS, David S (2001) MIP-1 alpha, MCP-1 GM-CSF, and TNF-alpha control the immune cell response that mediates rapid phagocytosis of myelin from the adult mouse spinal cord. J Neurosci 21(13):4649–4656
39. Aguirre A, Dupree JL, Mangin JM, Gallo V (2007) A functional role for EGFR signaling in myelination and remyelination. Nat Neurosci 10(8):990–1002
40. Aguirre A, Rubio ME, Gallo V (2010) Notch and EGFR pathway interaction regulates neural stem cell number and self-renewal. Nature 467(7313):323–327
41. Allamargot C, Pouplard-Barthelaix A, Fressinaud C (2001) A single intracerebral microinjection of platelet-derived growth factor (PDGF) accelerates the rate of remyelination in vivo. Brain Res 918(1–2):28–39
42. Carbajal KS, Schaumburg C, Strieter R, Kane J, Lane TE (2010) Migration of engrafted neural stem cells is mediated by CXCL12 signaling through CXCR4 in a viral model of multiple sclerosis. Proc Natl Acad Sci USA 107(24):11068–11073
43. Jean I, Allamargot C, Barthelaix-Pouplard A, Fressinaud C (2002) Axonal lesions and PDGF-enhanced remyelination in the rat corpus callosum after lysolecithin demyelination. Neuroreport 13(5):627–631
44. Murtie JC, Zhou YX, Le TQ, Vana AC, Armstrong RC (2005) PDGF and FGF2 pathways regulate distinct oligodendrocyte lineage responses in experimental demyelination with spontaneous remyelination. Neurobiol Dis 19(1–2):171–182
45. Patel JR, McCandless EE, Dorsey D, Klein RS (2010) CXCR4 promotes differentiation of oligodendrocyte progenitors and remyelination. Proc Natl Acad Sci USA 107(24):11062–11067
46. Doetsch F (2003) A niche for adult neural stem cells. Curr Opin Genet Dev 13(5):543–550
47. Kang SH, Fukaya M, Yang JK, Rothstein JD, Bergles DE (2010) NG2 + CNS glial progenitors remain committed to the oligodendrocyte lineage in postnatal life and following neurodegeneration. Neuron 68(4):668–681
48. Windrem MS, Nunes MC, Rashbaum WK, Schwartz TH, Goodman RA, McKhann G 2nd, Roy NS, Goldman SA (2004) Fetal and adult human oligodendrocyte progenitor cell isolates myelinate the congenitally dysmyelinated brain. Nat Med 10(1):93–97
49. Windrem MS, Schanz SJ, Guo M, Tian GF, Washco V, Stanwood N, Rasband M, Roy NS, Nedergaard M, Havton LA, Wang S, Goldman SA (2008) Neonatal chimerization with human glial progenitor cells can both remyelinate and rescue the otherwise lethally hypomyelinated shiverer mouse. Cell Stem Cell 2(6):553–565
50. Ray A, Mann MK, Basu S, Dittel BN (2011) A case for regulatory B cells in controlling the severity of autoimmune-mediated inflammation in experimental autoimmune encephalomyelitis and multiple sclerosis. J Neuroimmunol 230(1–2):1–9
51. Gadea A, Schinelli S, Gallo V (2008) Endothelin-1 regulates astrocyte proliferation and reactive gliosis via a JNK/c-Jun signaling pathway. J Neurosci 28(10):2394–2408
52. Foote AK, Blakemore WF (2005) Inflammation stimulates remyelination in areas of chronic demyelination. Brain 128(Pt 3):528–539
53. Woodruff RH, Franklin RJ (1999) Demyelination and remyelination of the caudal cerebellar peduncle of adult rats following stereotaxic injections of lysolecithin ethidium bromide, and complement/anti-galactocerebroside: a comparative study. Glia 25(3):216–228
54. Capone C, Frigerio S, Fumagalli S, Gelati M, Principato MC, Storini C, Montinaro M, Kraftsik R, De Curtis M, Parati E, De Simoni MG (2007) Neurosphere-derived cells exert a neuroprotective action by changing the ischemic microenvironment. PLoS One 2(4):e373
55. Kelly S, Bliss TM, Shah AK, Sun GH, Ma M, Foo WC, Masel J, Yenari MA, Weissman IL, Uchida N, Palmer T, Steinberg GK (2004) Transplanted human fetal neural stem cells survive migrate, and differentiate in ischemic rat cerebral cortex. Proc Natl Acad Sci USA 101(32):11839–11844
56. Aboody KS, Najbauer J, Danks MK (2008) Stem and progenitor cell-mediated tumor selective gene therapy. Gene Ther 15(10): 739–752
57. Rivers LE, Young KM, Rizzi M, Jamen F, Psachoulia K, Wade A, Kessaris N, Richardson WD (2008) PDGFRA/NG2 glia generate myelinating oligodendrocytes and piriform projection neurons in adult mice. Nat Neurosci 11(12):1392–1401
58. Corsini NS, Sancho-Martinez I, Laudenklos S, Glagow D, Kumar S, Letellier E, Koch P, Teodorczyk M, Kleber S, Klussmann S, Wiestler B, Brustle O, Mueller W, Gieffers C, Hill O, Thiemann M, Seedorf M, Gretz N, Sprengel R, Celikel T, Martin-Villalba A (2009) The death receptor CD95 activates adult neural stem cells for working memory formation and brain repair. Cell Stem Cell 5(2):178–190

59. Chandran S, Compston A, Jauniaux E, Gilson J, Blakemore W, Svendsen C (2004) Differential generation of oligodendrocytes from human and rodent embryonic spinal cord neural precursors. Glia 47(4):314–324
60. Targett MP, Sussman J, Scolding N, O'Leary MT, Compston DA, Blakemore WF (1996) Failure to achieve remyelination of demyelinated rat axons following transplantation of glial cells obtained from the adult human brain. Neuropathol Appl Neurobiol 22(3):199–206
61. Maciaczyk J, Singec I, Maciaczyk D, Klein A, Nikkhah G (2009) Restricted spontaneous in vitro differentiation and region-specific migration of long-term expanded fetal human neural precursor cells after transplantation into the adult rat brain. Stem Cells Dev 18(7):1043–1058
62. Maire CL, Buchet D, Kerninon C, Deboux C, Van Baron Evercooren A, Nait-Oumesmar B (2009) Directing human neural stem/precursor cells into oligodendrocytes by overexpression of Olig2 transcription factor. J Neurosci Res 87(15):3438–3446
63. Lindvall O, Bjorklund A (2004) Cell replacement therapy: helping the brain to repair itself. NeuroRx 1(4):379–381
64. Fagel DM, Ganat Y, Silbereis J, Ebbitt T, Stewart W, Zhang H, Ment LR, Vaccarino FM (2006) Cortical neurogenesis enhanced by chronic perinatal hypoxia. Exp Neurol 199(1):77–91
65. Parent JM, Valentin VV, Lowenstein DH (2002) Prolonged seizures increase proliferating neuroblasts in the adult rat sub-ventricular zone-olfactory bulb pathway. J Neurosci 22(8):3174–3188
66. Pluchino S, Zanotti L, Rossi B, Brambilla E, Ottoboni L, Salani G, Martinello M, Cattalini A, Bergami A, Furlan R, Comi G, Constantin G, Martino G (2005) Neurosphere-derived multipotent precursors promote neuroprotection by an immunomodulatory mechanism. Nature 436(7048):266–271